Natural Reference Targets in PALSAR-2 Interferometric Observations of Snow Covers Dynamics

Alexander Zakharov, Kotelnikov IRE RAS, aizakhar@sunclass.ire.rssi.ru, Russia
Ludmila Zakharova, Kotelnikov IRE RAS, ludmila@sunclass.ire.rssi.ru, Russia
Tumen Chimitdorzhiev, IPMS SB RAS, tchimit@gmail.com, Russia
Pavel Dagurov, IPMS SB RAS, pdagurov@gmail.com, Russia

Abstract

An efficiency of natural permanent scatterers like as power lines towers and engineering constructions in urban territories as reference targets in interferometric observations of snow covers dynamics on PALSAR-2 images Selenga river delta in Buryatia is studied. The discrepancy between signals of snow-free reference targets and surrounding fields occurs in the case of snowfall between the subsequent SAR observations constituting interferometric pair. From the processing of 3 adjacent PALSAR-2 interferometric pairs the snow layer increment up to 26 cm was detected, what is in a good agreement with measurements of local meteorological station.

1 Introduction

Snow covers state is important environmental parameter from both scientific and application oriented points of view. Remote sensing techniques, especially SAR based ones provide large scale and detailed mapping of snow covers. Capability of wet snow mapping with SAR was successfully demonstrated in C-band [1, 2]. Interferometric coherence is an indicator allowing the separation and mapping of wet snow extent from bare soils [3]. Dry snow is transparent medium: C-band signal penetrates up to 10 m in cold and dry firn, and L-band signal penetration is 5-10 m larger [4]. As dry snow is refractive medium, it is possible to use SAR differential interferometry measurements for the estimations of snow water equivalent and monitoring the dynamics of scattering surfaces beneath the snow and signal propagation trace state [5]. As an unknown initial phase on the interferogram introduces bias in phase measurements, it is mandatory to use known stable snow-free reference objects that provide calibration of phase measurements. The goal of this study is an attempt to monitor the dynamics of snow layer accumulation in vast plains of Selenga river delta in the end of 2014 - beginning of 2015 and to estimate snow layer thickness. Natural permanent scatterers like as power lines towers (see image in **Figure 1**) and engineering constructions near the Kamensk settlement, Buryatia, were chosen as reference targets.

By now similar studies were conducted mostly with SAR data acquired in higher frequency bands (C-band) [2], with natural consequence in a form of noisy results because of long orbit repetition interval and high temporal decorrelation of backscatter.

Figure 1: An example of one of the reference targets, power line towers near Kamensk settlement, Buryatia.

2 Data Description

Experimental data used in our study are Japanese PALSAR-2 L-band SAR data acquired at HH polarization over the Selenga river delta in the end of 2014 - beginning of 2015. Incidence angle of PALSAR-2 signal is θ=40°, slant range till the frame center r_n=750 km, pixel spacing in slant range δr=4.3 m, pixel spacing in azimuth δ_{az}=3.2 m. An example of the image fragment and interferogram with towers is presented in **Figure 2** and **Figure 3**. The satellite is on the left side of the image and moves in vertical direction. A series of white horizontal stripes in the upper part of the amplitude image are towers from **Figure 1**. Because of the layover effect, the backscattered signal of tower top has lower delay than that from its base, so, it is closer to the satellite. Average length of the tower in slant range is about 6-8 pixels, consequently, the altitude of the scatterers on the tower top is 30-35 m.

In the lower part of the image there are bright signatures of residential quartiers of Kamensk settlement. In the

ISBN 978-3-8007-4636-1 / ISSN 2197-4403

interferogram one can see dark vertical lines corresponding to bright echoes of residential quartiers on amplitude image.

Figure 2: Amplitude image of the test area acquired on November 24, 2014.

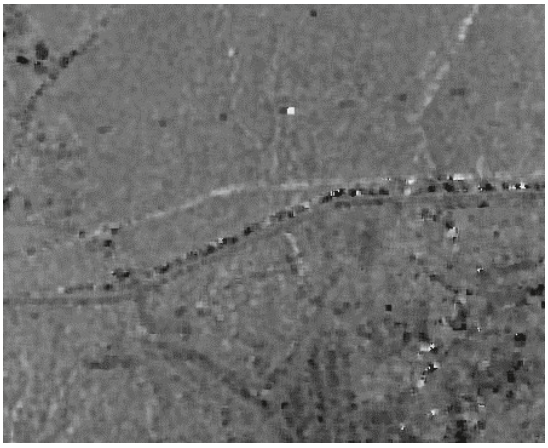

Figure 3: Interferogram for a November 24, 2014 - December 8, 2014 pair.

3 Data Analysis

Scheme of signals backscatter from a tower is shown in **Figure 4**. Surface scattering is typical for the backscatter from a tower top (point H). Signals undergo double-bounce scattering from dihedral reflector constituted by horizontal plain surface and vertical structure of tower (point B). Surface backscattering in the point A is typical for the surrounding plain area. Analysis of PALSAR polarimetric data confirms presence of the scattering mechanisms mentioned.

Snow layer S (dashed line in a **Figure 4**), formed as a result of snowfall between repeated SAR observations, affects the signal propagation conditions in the second observation, it extends electrical path length of signals traveling to the points A and B. On the interferogram from **Figure 3** dark pixels mark lower phase difference value and, respectively, shorter distance till the scattering point H compared with surrounding snow covered plains.

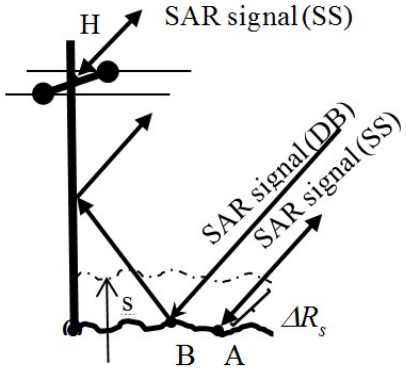

Figure 4: Mechanisms of the signal backscatter by power line tower elements.

Interferometric phase difference $\Delta\varphi_{12} = \varphi_1 - \varphi_2$ is a function $\Delta\varphi_t(\Delta h)$ topographic heights variations Δh or topographic phase, small-scale surface displacements (surface dynamics) $\Delta\varphi_d$ between first and second SAR observations, atmospheric fluctuations of signal path $\Delta\varphi_a$, system thermal noise $\Delta\varphi_n$ and unknown initial pahse difference $\Delta\varphi_0$. Lets enter the phase term describing influence of snow layer $\Delta\varphi_s$ [6]:

$$\Delta\varphi_{12} = \Delta\varphi_t + \Delta\varphi_s + \Delta\varphi_d + \Delta\varphi_a + \Delta\varphi_n + \Delta\varphi_0 \quad (1)$$

Topographic phase may be ignored because of large height ambiguity, typically exceeding 500 m in the case of PALSAR-2. Surface dynamics – frost heave or soil subsidence near the reference targets selected are unlikely, consequently, we may omit $\Delta\varphi_d$ also. Atmospheric effects may be ignored also as the test area is small enough compared with probable tropospheric geterogeneities. Initial phase $\Delta\varphi_0$ may be omitted also as we will work with double phase difefernces – between towers top and surrounding ground (for example, in the point A) $\Delta\varphi_{12H} - \Delta\varphi_{12A}$. Geometrical length of signal path in snow layer is ΔR_S. Increment of signal electrical path length because of snow layer formed between sessions 1 and 2 may expressed as

$$\Delta l_{12S} = \frac{\Delta\varphi_{12H} - \Delta\varphi_{12A}}{4\pi}\lambda . \quad (2)$$

Five interferometric pairs mentioned in Table 1 used to calculate double differences $\Delta\varphi_{12H} - \Delta\varphi_{12A}$ for 13 power line towers. Increment of signal path length Δl here is average value for the towers mentioned.

Some meteorological information for the October 01, 2014 – February 28, 2015 interval is shown on a plot in **Figure 5** [8]. During first interval (starting from October 22), daily temperature was negative mainly. Permanent snow cover formation started on November 19. According to the data from **Table 1**, on the first

ISBN 978-3-8007-4636-1 / ISSN 2197-4403

interval of interferometric observations there was 0.1 cm increase of signal path, -0.1 cm on the second interval, 2.1 cm on the third interval, 3.3 cm on the fourth and 1.2 cm on the last interval. Total path increase on the intervals 3-5 (November 24, 2014 – January 19, 2015), covering 8 weeks of snow accumulation, is 6.6 cm. A plot of cumulative increments of signal path in snow covers on the intervals 3, 3+4 and 3+4+5 for each of 13 towers shown in **Figure 6**.

We measured also increments of signal path length for the signals with double-bounce backscatter inserting phase $\Delta\varphi_{12B}$ of double bounce signal (scattered in the point B) instead of $\Delta\varphi_{12H}$ for signal with surface scattering in (2). As expected, these increments are zero, on average and will not be mentioned later.

Pair/ Interval	Dates	Height amb., m	Δl, cm
1	141022-141105	-447	-0.1
2	141105-141119	1000	0.1
3	141124-141208	-466	2.1
4	141208-141222	-553	3.3
5	141222-150119	-1000	1.2

Table 1: Mean increments of signal path Δl.

As it is known, the increment in the signal path length in the snow layer may be linked to the thickness of the snow cover [5]. For a one-way increment Δl and snow thickness s from [5, 7]:

$$s = -\frac{\Delta l}{(\cos\theta - \sqrt{\varepsilon_s - \sin^2\theta})}. \qquad (3)$$

Dielectric permittivity of dry snow ε_s is linked with its density ρ_d [5]:

$$\varepsilon_s = 1 + 1.6\rho_d + 1.86\rho_d^3.$$

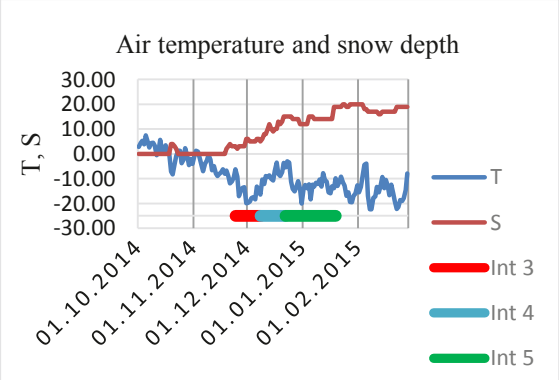

Figure 5: Air temperature, degrees, and snow depth, cm, during 01.10.2014-28.02.2015.

For the most probable snow density ρ_d =0.25 in mid-winter the dielectric permittivity ε_s =1.53. Snow thickness, evaluated from (3), is 26 cm, what is consistent with nearby Kabansk ground meteorological station метеостанции. The discrepancy observed may be explained by snow hardening during winter time with subsequent increase of snow density.

It is necessary to underline that 6.6 cm increment of signal path on 2 month interval is much less than 24.2 cm phase ambiguity interval. Consequently, maximal repeat interval between interferometric observations may be in our case longer than 2 months provided the accumulated snow depth is less than 1 m. The restriction on the repeat interval length is much more severe in C and X-band SAR, where the wavelengths are 4 and 8 times shorter and temporal decorrelation is significantly higher.

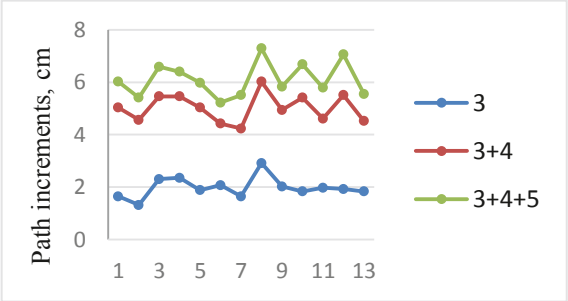

Figure 6: Increments of Δl in snow layer according to echoes of 13 towers in 24.11.2014-19.01.2015.

Similar manifestation of the snow fall may be observed in urban territories. In a lower part of **Figures 2 and 3** there are residential quarters in Kamensk settlement. Obviously, snow free territories near the buildings along with vertical walls provide double-bounce backscatter, which is free from snow induced phase shift, which can be observed in surrounding fields provided there was snowfall between the observations. The same was found to be true for a strong point-like backscatter from cathedral in Posolsk settlement (see amplitude image and interferogram in **Figure 7**).

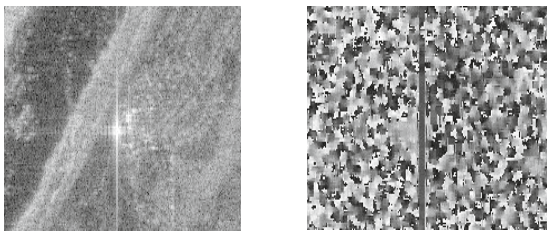

Figure 7: Amplitude image (left) and interferogram (right) of cathedral in Posolsk settlement.

It necessary to underline, that there is no such a prominent phase deviation on the PALSAR-2

ISBN 978-3-8007-4636-1 / ISSN 2197-4403

interferograms in the places mentioned during snow free periods.

Unlike the residential quartiers in large settlements, sparse small country houses in Istomino settlement (not shown here) seem to be useless for the phase calibration purposes. Though they demonstrate strong point-like backscatter, there is no deviation of phase compared with phase of backscatter from surrounding plain areas. Probable explanation is that the phase of signal scattered from snow-covered roofs in single scattering scheme is affected by snow layer in similar way as in the fields.

The difference between measurements of cumulative increments of signal path during 3 subsequent time intervals 3-5 from **Table 1** using power line towers and residential quartiers is given in **Figure 8** below.

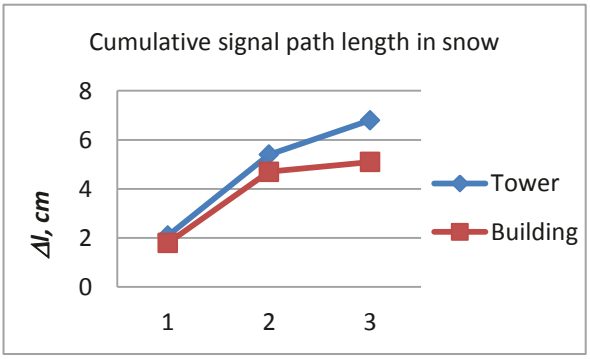

Figure 8: Cumulative increments of signal path length in schemes with towers and buildings on 3 successive interferometric intervals of observations.

Though there is 2 cm underestimation of signal path in residential area, rows of residential buildings in large settlements (as well as other engineering constructions like as cathedral in one of examples presented above) may be also used as reference targets in phase calibration. The discrepancy between the plots may be explained by an impact of residual snow layer on the streets near the buildings, which may introduce corrupting phase shift in the case of signal double bounce backscatter from dihedral "building wall - street surface".

4 Conclusions

Radar interferometry is a powerful tool for the monitoring of dry snow accumulation, allowing the estimation of its thickness and snow water equivalent (SWE) [5]. Various natural reference targets (power line towers, buildings of residential quartiers, etc) may be used for a phase calibration in differential radar interferometry scheme for snow layer thickness and SWE estimations. L-band SAR data are preferable compared with C and X-band because of longer ambiguity interval and lower temporal decorrelation. PALSAR-2 measurements are of especial value because of the shortest (two weeks) repeat orbit interval.

Acknowledgments

Authors are grateful for support of Russian Foundation of Basic Research (projects N15-29-06003, N18-07-00816) and to JAXA for the provision of PALSAR-2 data under the project RA4-331.

References

[1] J.T. Koskinen, J. Pulliainen, and M. Hallikainen, *The use of ERS-1 SAR data in snow melt monitoring*, IEEE Trans. Geosci. Remote Sensing, vol. 35, pp. 601–610, Mar. 1997.

[2] T. Guneriussen, H. Johnsen, and I. Lauknes, *Snow cover mapping capabilities using RADARSAT standard mode data*, Can. J. Remote Sensing, vol. 27, pp. 109–117, Nov. 1999

[3] J. Shi, J. Dozier, and S. Hensley, *Mapping snow cover with repeat pass synthetic aperture radar*, *IEEE Proc. IGARSS'97*, Singapore, 1997, pp. 628–630

[4] E. Rignot, K. Echelmeyer, and W. Krabill, *Penetration depth of interferometric synthetic-aperture radar signals in snow and ice*, Geophys. Res. Lett., vol. 28, no. 18, pp. 3501–3504, 2001

[5] T. Guneriussen, K. Høgda, H. Johnsen, I. Lauknes, *InSAR for estimation of changes in snow water equivalent of dry snow*, IEEE Trans. Geosci. and Remote Sens., 39(10), October 2001, pp. 2101–2108, 2001

[6] A.I. Zakharov, O.I. Yakovlev, V.M. Smirnov, *Sputnikoviy monitoring Zemli. Radiolokatsionnoe zondirovanie poverhnosti (Satellite Earth observation, Radar remote sensing of the surface)*. Moscow: KRASAND, 248 p., 2012.

[7] S. Leinss, A. Wiesmann, J. Lemmetyinen, I. Hajnsek, *Snow water equivalent of dry snow measured by differential interferometry*, IEEE J. Sel. Topics Appl. Earth Observ. Remote Sens., vol. 8, no. 8, Aug. 2015, pp. 3773–3790.

[8] https://rp5.ru/

